ELSEVIER

International Journal of Coal Geology 51 (2002) 237–250

International Journal of COAL GEOLOGY

www.elsevier.com/locate/ijcoalgeo

Distribution, isotopic variation and origin of sulfur in coals in the Wuda coalfield, Inner Mongolia, China

Shifeng Dai *, Deyi Ren, Yuegang Tang, Longyi Shao, Shengsheng Li

China University of Mining and Technology, Box 1, D11, Xueyuan Road, Haidian District, Beijing 100083, China

Received 15 November 2001; accepted 29 April 2002

Abstract

This paper describes coal petrographic characteristics, sulfur abundance, distribution and isotopic signature in coals in the Wuda coalfield, Inner Mongolia, northern China. Petrographic studies suggest that depositional environment influences petrographic composition. The No. 9 and No. 10 coal seams, which are thought to have formed on a tidal delta plain, have high collodetrinite contents (up to 66.1%) indicating enhanced gelification and bacteria activity during coal accumulation, and also have the highest sulfur content (3.46% and 3.42%). Both organic and pyritic sulfur isotope values (− 12.3 ‰ to 5.8 ‰ and − 18.7 ‰ to 1.1 ‰, respectively) are variable and generally tend to be more negative in high-sulfur coals than those in low-sulfur coals in the Wuda coalfield. The negative sulfur isotope values indicate that a large portion of sulfur in the high-sulfur coals has a bacterial origin. Sulfur isotopic compositions and variations within the section were used to propose a model to explain the origin of sulfur in these coals. The presence of pyritized rod-like bacteria, cyanophyte's gelatinous sheaths and degraded algae organic matter suggests that bacteria, and perhaps algae, may play an important role in the formation of these high-sulfur coals.

Keywords: Coal petrology; Organic sulfur; Pyrite; Sulfur isotopes; Rod-like bacteria; Algae

1. Introduction

Information about the abundance, distribution and origin of sulfur in coals is important in coal combustion because the sulfur oxides released can be a major source of acid rain. Many researchers have investigated sulfur in coals, including sulfur distribution, origin and mechanisms of the sulfur incorporation into coals (for example, Smith and Batts, 1974; Casagrande and Price, 1981; Smith et al., 1981; Love et al., 1983; Lyons et al., 1989; Price and Casagrande, 1991; Tang and Ren, 1993; Spiker et al., 1994; Whateley and Tuncali, 1995; Kostava et al., 1996; Gayer et al., 1999; Dai, 2000). Variation in sulfur content of coal is controlled mainly by geological conditions. Sulfur available during plant growth is the principal source of sulfur in low-sulfur coal, and the $\delta^{34}S$ values of organic sulfur range from 2 ‰ to 8 ‰ (Chou, 1997). In contrast, in medium- (1–3% total sulfur) and high-sulfur (>3% total sulfur) coals overlain by a marine roof, most of the sulfur is derived from seawater sulfate (Diessel, 1992; Chou, 1997). Bacterial reduction of sulfate produces H_2S, which

* Corresponding author. Tel.: +86-10-62331293; fax: +86-10-62325016.

E-mail address: dsf@cumtb.edu.cn (S. Dai).

0166-5162/02/$ - see front matter © 2002 Elsevier Science B.V. All rights reserved.
PII: S0166-5162(02)00098-8

reacts with organic matter during early diagenesis to form sulfides and organosulfur compounds. The most obvious source of sulfate in coastal peat swamp is seawater. In general, the $\delta^{34}S$ values in medium- and high-sulfur coals are variable, suggesting microbiological isotopic fractionation. The large kinetic isotope fractionation that accompanies bacterial sulfate reduction generally produces sulfides with $\delta^{34}S$ values 15–40‰ lower than that of the reactant sulfate (Price and Shieh, 1979). Where sulfate concentrations remain low and limited during early diagenesis, such as in nonmarine environments, near-quantitative bacterial reduction of all the available sulfate results in the addition of comparatively ^{34}S-rich sulfur species to the coal. $\delta^{34}S$ values greater than 20‰ are not uncommon in low-sulfur coals with nonmarine roof rocks (Price and Shieh, 1979; Westgate and Anderson, 1984). Thiols, sulfides and disulfides, and thiophene and its derivatives are thought to be several kinds of organic sulfur compounds that occur in coals (Dai, 2000).

The Wuda coalfield is one of the major coking coal mining areas in North China. The No. 9 and No. 10 coal seams in this coalfield have high sulfur contents (3.46% and 3.42%, respectively) and this sulfur influences the quality of coke manufacture. In this paper, we discuss petrographic composition of coals, the abundance of organic sulfur, and the compositions of sulfur isotopes, and then put forward a model of sulfur origin for the Wuda coals.

2. Geological setting

The Wuda coalfield is located in northern China and consists of coal-bearing strata of Pennsylvanian

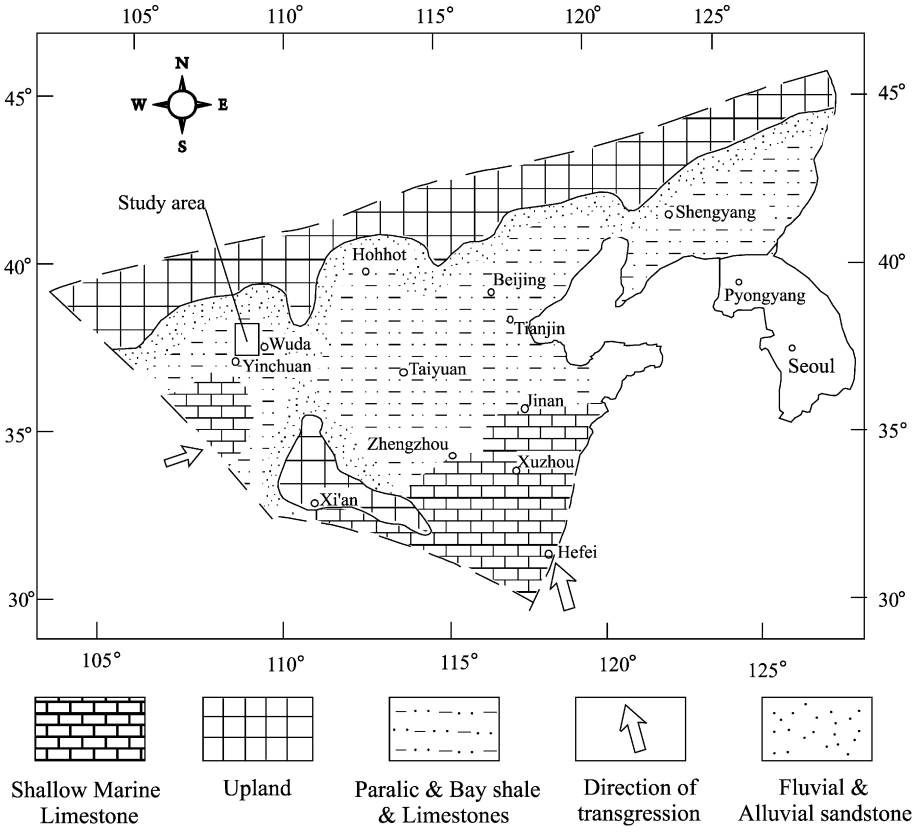

Fig. 1. Location of the Wuda coalfield and the paleogeography of Late Paleozoic in North China (modified after Han and Yang, 1980 and Liu, 1990).

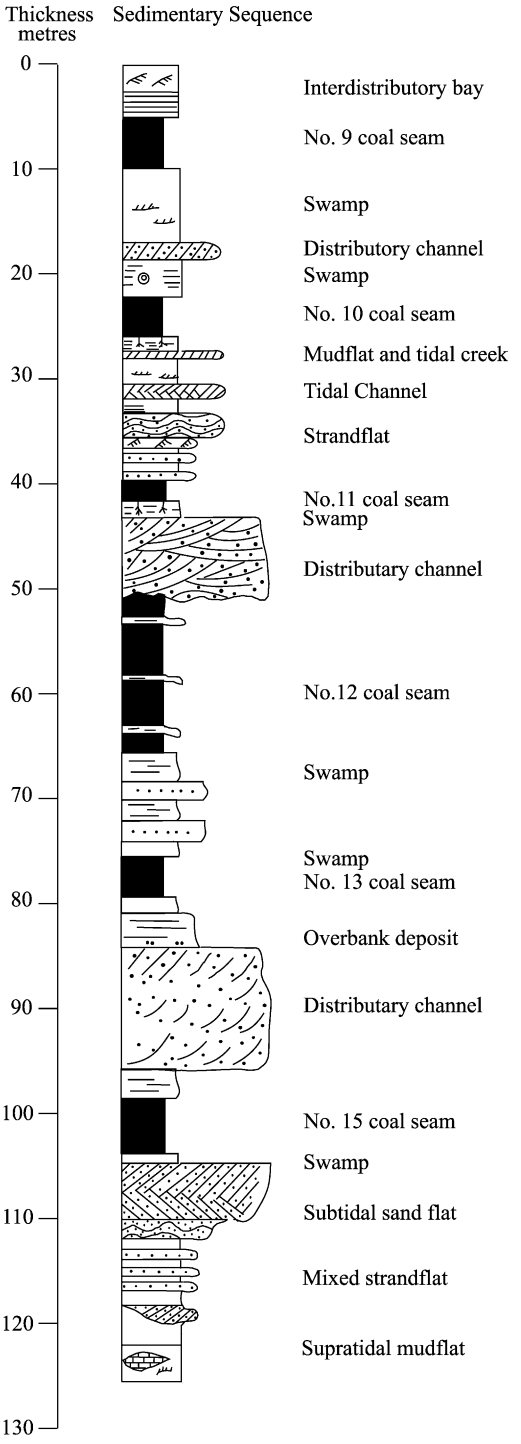

Fig. 2. Sedimentary sequence of coal seams in Pennsylvanian Taiyuan Formation.

and Permian ages. Approximately 80% of the coal mined in China comes from Pennsylvanian coal seams. The paleogeography of Late Paleozoic in North China ranged successively from upland through alluvial and fluvial plain, paralic delta and tidal flat (sometimes tidal flat-barrier complex) to shallow marine (Fig. 1). The paleogeography and lithofacies of Pennsylvanian in North China can be divided into three belts (Han and Yang, 1980; Liu, 1990). In the northern belt, north of the line linking Yinchuan and Beijing (see locations in Fig. 1), the Taiyuan Formation is dominated by clastics; the ratio of clastics versus carbonate and coal is 8:1 (Han and Yang, 1980). In the southern belt, south of Zhengzhou, the sediments are dominated by limestone, which has a thickness of 30–50 m, and comprise 50–70% of the total thickness. In the central belt, the sediments are characterized by alternating fine clastics and limestones, suggesting a shifting shoreline zone (Liu, 1990). The Wuda coalfield is located in the northern part of this central belt (Fig. 1).

Pennsylvanian coal-bearing strata in the Wuda coalfield include the Pennsylvanian Benxi Formation (C_{2b}), the Pennsylvanian Taiyuan Formation (C_{2t}), the Early Permian Shanxi Formation (P_{1s}) and Xiashihezi Formation (P_{1x}), and the Late Permian Shangshihezi Formation (P_{2sh}). The Taiyuan Formation is the major coal-bearing formation which consists of sandstone, limestone, mudstone and coal (No. 9, No. 10, No. 12, No. 13 and No. 15 coal seams), with a thickness between 70 and 140 m decreasing from the center towards both the south and north. The No. 15 coal seam was formed in a tidal plain setting, and the No. 13 and No. 12 coal seams were formed in a fluvial delta plain setting, and the No. 10 and No. 9 coal seams were formed in a tidal delta plain setting (Fig. 2) (Peng and Zhang, 1995).

3. Methods of study

A total of 157 coal-seam channel samples was collected from the No. 9, No. 10, No. 12, No. 13 and No. 15 coal seams of the Taiyuan Formation. In addition, macroscopically recognizable plies of the No. 9 (13 samples) and the No. 13 (six samples) coal seams were collected. Samples of each ply approximately 15 cm across and 10 cm deep were taken from

mined faces to ensure as little contamination as possible from mine operations and to minimize oxidation effects on the samples.

For petrographic study, each sample was ground to a maximum particle size of 850 μm, and formed into two coal pellets with an epoxy resin binder. The guidelines and laboratory procedures for preparing and polishing the pellets conform to ASTM (1997). Constituents were identified using both white- and UV-light reflectance microscopy and more than 500 counts were measured for each polished pellet. The analytical results from both pellets for each sample were compared to ensure that they were within 2% mean variation according to standard ASTM techniques (ASTM, 1997). Average petrographic composition for coal-seam channel samples is shown in Table 1. Mean maximum reflectance of vitrinite (%$R_{o,max}$) was based on at least 50 measurements collected using a Leitz MPVIII photometer system. For chemical analysis, samples were crushed and ground to less than 60 mesh. Forms of sulfur were determined according to ASTM standard (1997).

The isotopic measurements were made at the Chemical Metallurgic Institute, Chinese Academy of Sciences (Delta Spectrometer System) and reported in the standard δ notation as per mil (‰) deviation in the $^{34}S/^{32}S$ ratio in the sample from the standard Canon Diablo Troilite. A scanning electron microscope (S360 SEM) fitted with an Oxford Instrument AN 10000 EDX analyzer, based at Beijing Petroleum Exploration Institute, was used to determine the organic sulfur content of individual coal macerals and to study the submicroscopic character of the coal. A transmission electron microscope (TEM), based at the Beijing Physicochemical Analysis Center, was used to study degraded algae organic matter.

4. Petrographic characteristics of the coal seams

All coal samples studied in the Wuda coalfield have low liptinite contents (Table 1), probably related to the coal rank. It also can be seen that the coal seams formed in the same sedimentary environments have similar

Table 1
Petrographic compositions of coal seams in the Wuda coalfield (vol.%)

Maceral	No. 9 coal seam		No. 10 coal seam		No. 12 coal seam		No. 13 coal seam		No. 15 coal seam	
	Average	Range	Average	Range	Average	Range	Average	Range	Average	Range
CD	52.4	39.0–64.7	50.0	34.2–60.4	42.7	27.1–55.3	44.1	27.5–57.7	48.1	34.0–50.2
CT	10.2	1.3–22.8	13.4	3.8–28.1	9.9	3.7–19.6	13.6	4.5–30.4	8.2	4.6–10.9
VD	3.2	0–28.31	0.9	0–2.59	2.7	0.8–5.8	0.8	0–3.8	1.3	0–4.2
CG	1.2	0–4.6	1.7	0.71–2.8	1.7	0.5–6.7	0.9	0–3.8	0.9	0–2.5
T	3.8	0–14.5	2.0	0–4.3	3.7	1.5–7.0	3.1	0.3–8.0	2.9	1.6–4.8
Total V	70.8		68.0		60.7		62.5		60.4	
Sp	0.4	0–1.0	0.3	0–0.8	0.3	0–0.8	0.2	0–0.9	0.1	0–0.4
Cu	0.2	0–0.4	0.2	0–1.5	0.5	0–1.0	0.4	0–1.6	0.2	0–1.2
Re			0.2	0–0.4	0.2	0–0.3				
Total L	0.6		0.7		1.0		0.6		0.3	
F	12.7	5.5–19.6	14.8	9.2–25.6	10.5	3.1–17.3	10.9	4.5–17.6	13.7	10.8–16.4
SF	5.8	3.3–9.5	5.6	2.3–9.7	4.3	1.3–9.6	4.4	1.5–9.6	8.0	5.9–14.5
Ma	0.5	0–2.4	0.7	0–1.7	0.9	0–3.0	0.7	0–2.4	0.9	0.4–1.7
Mi	1.0	0–5.6	0.8	0–6.2	0.9	0–3.1	0.9	0–2.9	1.3	0–5.4
ID	2.5	0–9.3	1.6	0.5–3.0	1.9	0.5–3.7	1.4	0–3.0	2.7	1.2–6.7
Total I	22.5		23.5		18.5		18.3		26.6	
Q	0.2	0–1.4	0.2	0–0.3	0.1	0–1.3	0.4	0–5.8	0.1	0–0.2
Py	2.5	0.2–7.3	2.7	0–12.2	1.2	0–5.8	0.7	0–1.7	1.5	0–7.6
Ca	0.2	0–0.6	0.2	0–1.5	0.6	0–3.8	0.5	0–2.4	0.5	0–3.0
Cl	3.2	0.8–13.0	4.7	1.0–9.6	17.9	5.1–37.4	17.0	9.6–31.6	10.6	0.2–17.7
Total M	6.1		7.8		19.8		18.6		12.7	

CD, collodetrinite; CT, collotelinite; VD, vitrodetrinite; CG, corpogelinite; T, telinite; Sp, sporinite; Cu, cutinite; Re, resinite; F, fusinite; SF, semifusinite; Ma, macrinite Mi, micrinite; ID, inertrodetrinite; Q, quartz; Py, pyrite; Ca, carbonates; Cl, clay minerals; V, Vitrinite; L, Liptinite; I, Inertinite; M, Mineral.

Table 2
Sulfur and ash content of different coal seams (based on 157 samples for each coal seam)

Coal seam	Depositional environment	$S_{t,d}$ (%)	$S_{p,d}$ (%)	$S_{s,d}$ (%)	$S_{o,d}$ (%)	Ash_d(%)	$R_{o,max}$(%)
No. 9	tidal delta plain	3.46	1.12	0.19	2.15	13.10	1.09
No. 10	tidal delta plain	3.42	1.06	0.24	2.02	19.67	1.10
No. 12	fluvial delta plain	2.29	0.41	0.41	1.47	23.39	1.12
No. 13	fluvial delta plain	0.88	0.22	0.12	0.54	23.92	1.14
No. 15	tidal flat	1.95	0.61	0.12	1.22	22.69	1.17

S_t, total sulfur; S_p, sulfide sulfur; S_s, sulfate sulfur; S_o, organic sulfur; $R_{o,max}$, mean maximum reflectance of vitrinite; d, dry base.

organic maceral and mineral compositions. Compared with other coal seams, No. 9 ($R_{o,max}$ = 1.09%) and No. 10 ($R_{o,max}$ = 1.10%) coal seams formed in tidal delta plains (Fig. 2) have the highest content of vitrinite (70.8% and 68.0%, respectively) and pyrite (2.5% and 2.7%, respectively), but the lowest content of total minerals. Moreover, vitrinites of the two coal seams are dominated by collodetrinite (52.4% and 50.0%, respectively). The No. 12 ($R_{o,max}$ = 1.12%) and No. 13 ($R_{o,max}$ = 1.14%) coal seams formed in fluvial delta plains (Fig. 2) have the highest mineral content (19.8% and 18.6%, respectively), but the lowest pyrite content (1.2% and 0.7%, respectively) because of the less seawater influences during peat accumulation; in other words, there are high contents of detrital materials of the terrigenous origin, especially the clay minerals. Relatively, the No. 15 coal seam ($R_{o,max}$ = 1.17%) formed on the basis of the tidal plain (Fig. 2) has a narrow variation of coal macerals (for example, collodetrinite with a content range from 34.0% to 50.2%) and the highest inertinite (average 26.6%) and the medium pyrite contents (1.5%).

5. Abundance, distribution and variation of organic sulfur in coal macerals

It is accepted that marine-influenced peats generally have higher sulfur contents than freshwater-influenced peats (Casagrande et al., 1977). The high sulfur contents (Table 2) in the No. 9 (3.46%), No. 10 (3.42%), No. 12 (2.29%) and No. 15 (1.95%) coal seams cannot be accounted for by the original plant sulfur. Therefore, there must have been some sulfur incorporated into peat after plants died and were buried.

It is difficult to determine the organic sulfur content of individual macerals using traditional chemical methods due to the small size of the macerals and their intimate relations with one another in most coals (Chou, 1990; Mastalerz and Bustin, 1993; Dai and Ren, 1996; Ward and Gurba, 1998). Raymond (1978) determined organic sulfur using an electron microprobe, a technique that allows the direct determination of the organic sulfur content of individual macerals.

The organic sulfur content of macerals of different coal seams was determined using scanning electron microscope (SEM) in conjunction with energy dispersive X-ray (EDX) spectrometer. The results (Table 3) show that organic sulfur content in macerals of the same coal sample decreases in the order: collodetrinite, corpogelinite, collotelinite, cutinite, semifusinite, macrinite, fusinite. These results are in accordance with those reported by Chou (1990) and Lei et al. (1995), except for the organic sulfur content in cutinite and sporinite.

Organic sulfur content is more variable in collodetrinite than that in collotelinite (Fig. 3a). Demir et al.

Table 3
Abundance and distribution of organic sulfur in macerals of different coals (%)

Coal seam	CD	CG	CT	T	Cu	F	SF	Ma	Sp
No. 9	1.71–3.73 (3.22)	2.76	1.74–2.20 (2.05)		1.89	1.24–2.28 (1.61)	1.75	1.73	
No. 10	1.96–2.08 (2.00)		1.71–1.99 (1.86)	1.82		1.00–1.09 (1.05)	1.31		1.98
No. 12	1.12–1.31 (1.22)	1.15		0.98–1.32 (1.10)		0.97		1.12	
No. 13	0.54–0.71 (0.68)					0.52	0.33		
No. 15	1.08–2.17 (1.32)		0.87			0.67–0.79 (0.74)	0.75		1.16

CD, collodetrinite; CG, corpogelinite; CT, collotelinite; T, telinite; Cu, cutinite; F, fusinite; SF, semifusinite; Ma, macrinite; Sp, sporinite.

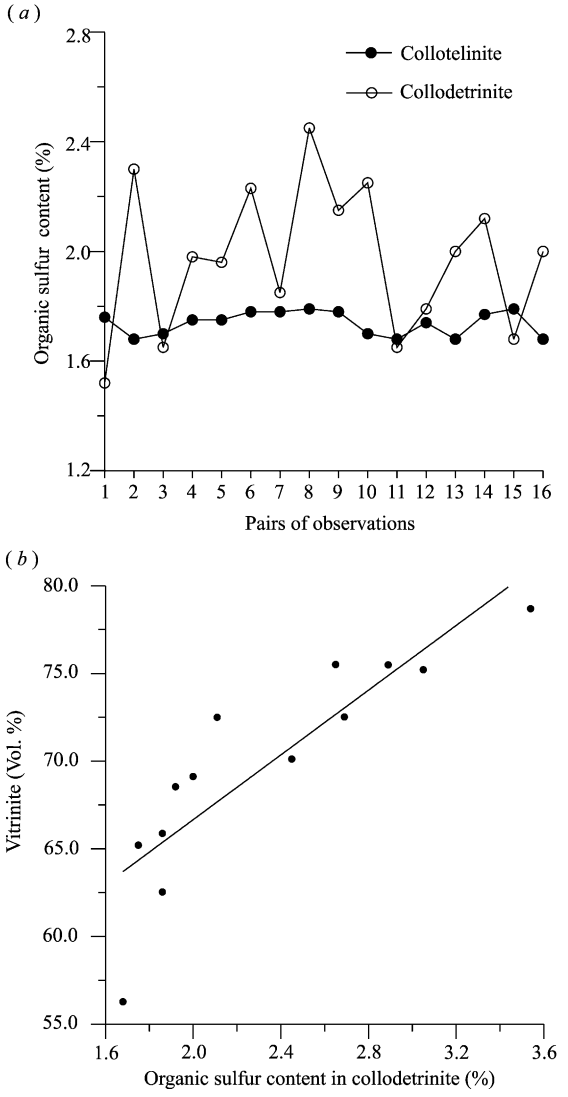

Fig. 3. Distribution of organic sulfur in the No. 9 coal seam. (a) Organic sulfur distribution in collodetrinite and collotelinite. (b) Relationship between organic sulfur content in collodetrinite and vitrinite groups.

(1993) suggested that the organic sulfur content of macerals depends on the difference of chemical structure in the maceral precursor. Compared with inertinite and liptinite, vitrinite, which is the predominant maceral group indicating the deep gelification degree, has the highest organic sulfur content (Tables 3 and 4), suggesting that there is a positive relationship between the organic sulfur content and the gelification degree.

Fig. 3b shows that there is also a positive relationship between organic sulfur content in collodetrinite and the vitrinite maceral group content in the No. 9 coal seam, and it can be concluded by default that there is a negative relationship between organic sulfur and the inertinite maceral family. The vitrinite precursors, especially the collodetrinite, formed in peat-forming environments in which the water table was high and Eh was low (Casagrande and Price, 1981). These conditions favored bacterial sulfate reduction and H_2S, which could then react with organic peat compounds to form organic sulfur components (Casagrande, 1981; Lei and Ren, 1995; Dai, 2000). In contrast, inertinite precursors formed where the water table was low and Eh was high. Aerobic respiration prevailed here and less H_2S was produced. In other words, the organic sulfur content is related to gelification degree.

6. Sulfur isotopic composition and model of sulfur origin

Sulfur isotopes can be used to interpret the origin of sulfur and provide important information on depositional environments of coal (Smith and Batts, 1974; Love et al., 1983; Passier et al., 1997). It is generally believed that the isotopic composition of pyritic sulfur is more variable than that of organic sulfur (Westgate and Anderson, 1984). The $\delta^{34}S$ values of freshwater peats from Okefenokee Swamp are higher than those of marine peats from the Florida Everglades (Casagrande, 1987). In this study, 13 plies for one columnar section of the No. 9 coal seam and six plies of the No. 13 coal seam have been analyzed for sulfur isotopes.

In the columnar section of the No. 9 coal seam, the major maceral group is vitrinite (except sample 9-7), with collodetrinite content up to 66.1% (Table 4). Relatively, the contents of fusinite, semifusinite, and macrinite are not high, but inertrodetrinite is common, especially in the middle of the section. Minerals in the No. 9 coal seam are dominated by clay minerals and pyrite, while quartz and carbonate contents are relatively low. These petrographic characteristics suggest a relatively strong gelification environment that results in an intense decomposition of coal macerals, and a turbulent medium condition that results in the formation of inertrodetrinite.

Table 4
Analysis of coal petrology and sulfur isotopes of the No. 9 and No. 13 coal seams

Samples	H (m)	S (%)				δ^{34}S (‰)		Vitrinite (vol.%)						Inertinite (vol.%)						Liptinite (vol.%)				Mineral (vol.%)				
		$S_{t,d}$	$S_{p,d}$	$S_{s,d}$	$S_{o,d}$	$\delta^{34}S_{py}$	$\delta^{34}S_{org}$	CD	CT	T	CG	VD	total	F	SF	Ma	Mi	ID	Total	Sp	Cu	Re	Total	Q	Py	Ca	Cl	Total
9-13	0.45	6.71	3.58	0.16	2.97	−18.7	−12.3	61.2	3.1	5.1	1.4	0.6	71.4	10.2	2.8	1.4	0.6	1.1	16.1	0.2	0.2		0.4	1.4	5.8	0.4	4.6	12.2
9-12	0.25	6.43	3.48	0.18	2.77	−15.6	–	52.7	3.2	4.3	0.3	1.6	62.1	16.3	8.6	1.6		3.4	29.9					0.2	3.6		5.2	9.0
9-11	0.37	4.46	2.46	0.20	1.80	−17.5	–	48.6	2.8			2.4	53.8	18.7	8.5	2.1	4.3	3.1	36.7		0.2		0.2		3.2	0.3	5.8	9.3
9-10	0.28	3.38	1.24	0.16	1.98	−12.3	−8.2	45.5	1.2	5.1	0.6	7.6	60.0	20.2	5.8			3.3	29.3		0.2		0.2	0.6	2.0	1.5	6.4	10.5
9-9	0.40	2.68	1.20	0.18	1.30	−9.6	–	57.2	1.6	0.8	0.2	6.4	66.2	16.5	3.4	3.6	0.5	5.4	29.4	0.2			0.2		2.6		1.5	4.1
9-8	0.34	2.46	1.08	0.17	1.21	−8.4	2.5	49.2	4.7		1.1	8.4	63.4	10.9	8.8		3.2	6.8	29.7						1.8		5.2	7.0
9-7	0.20	2.52	0.40	0.21	1.91	0.9	–	24.6	2.4	0.8		5.7	33.5	27.6	9.5	2.4	5.6	9.3	54.4					2.7	0.6	0.4	8.4	12.1
9-6	0.32	2.18	0.41	0.22	1.55	1.1	5.8	28.4	5.3		2.4	11.5	47.6	24.1	7.4	1.8	4.2	8.5	46.0	0.3			0.3	0.5	0.8		4.8	6.1
9-5	0.30	2.52	0.72	0.14	1.66	−2.4	–	42.5	4.5	10.2		6.8	64.0	16.4	5.8		0.8	6.7	29.7	0.2			0.2	0.2	1.4		4.6	6.2
9-4	0.35	2.37	1.44	0.18	0.75	−5.6	−2.4	33.2	8.7	8.4	4.9	8.5	63.7	22.4	1.5	5.7			29.6	0.2			0.2		3.8		2.7	6.5
9-3	0.46	2.90	0.81	0.20	1.89	−8.9	–	42.6	11.4	0.6	2.4	8.6	65.6	20.1	6.4		0.4	1.9	28.8	0.4			0.4	1.0	1.6		2.6	5.2
9-2	0.28	2.93	1.46	0.18	1.29	−7.8	–	66.1	5.4		1.8	6.4	79.7	9.8	3.5			1.9	15.2					0.3	2.4		1.8	4.5
9-1	0.34	3.62	1.36	0.17	2.09	−12.4	−6.4	60.3	10.4	0.8	2.1	0.8	74.4	11.6	2.4	2.4		4.5	20.9	0.2	0.2		0.4		3.6	0.4	2.5	6.5
13-6	0.72	0.84	0.31	0.09	0.44	–	11.5	46.0	13.5	3.8	0.8		64.1	18.2	3.4	1.2	0.5	1.3	24.6	0.6	0.2		0.8	0.2	0.5		9.8	10.5
13-5	0.58	0.85	0.45	0.1	0.3	8.6	9.8	40.6	8.4	5.6	0.6	0.6	55.8	7.6	3.0	0.3		8.6	19.5	0.9	0.3	0.2	1.4	0.2	0.6	0.4	21.5	22.7
13-4	0.72	0.90	0.35	0.12	0.43	–	9.6	21.9	10.6	11.4	2.4	0.4	46.7	9.8	5.9			2.4	18.1	0.6	1.0		1.6	4.9	0.8	2.2	25.7	33.6
13-3	0.54	0.69	0.18	0.08	0.43	–	10.4	10.8	22.8	8.8	3.6	1.8	47.8	10.4	1.4	2.6		2.8	17.2	0.6	1.4		2.0	1.0	0.2		20.6	21.8
13-2	0.70	0.78	0.54	0.13	0.11	8.3	8.9	24.8	16.4	10.3	1.5	2.2	55.2	14.6	2.6			1.4	18.6	0.8	0.4		1.2	4.2	0.6		20.3	25.1
13-1	0.66	0.89	0.44	0.08	0.37	9.7	11.2	51.3	11.6	2.4	1.2	0.6	67.1	11.2	0.8	2.6		2.6	17.2						0.5	0.4	14.8	15.7

H, thickness; 9-1, . . ., 9-13, columnar section of No. 9 coal seam; 13-1, . . ., 13-6, columnar section of No. 13 coal seam; $\delta^{34}S_{py}$, $\delta^{34}S$ value of pyrite; $\delta^{34}S_{org}$, ^{34}S value of organic sulfur; CD, collodetrinite; CT, collotelinite; VD, vitrodetrinite; CG, corpogelinite; T, telinite; Sp, sporinite; Cu, cutinite; Re, resinite; F, fusinite; SF, semifusinite; Ma, macrinite Mi, micrinite; ID, inertrodetrinite; Q, quartz; Py, pyrite; Ca, carbonates; Cl, clay minerals; S_t, total sulfur; S_p, sulfide sulfur; S_s, sulfate sulfur; S_o, organic sulfur; d, dry base.

Both the organic sulfur and pyritic sulfur in the No. 13 coal seam (which contains less than 1% total sulfur) have a narrow range in isotopic composition, 9.6–11.5‰ and 8.6–9.7‰, respectively, whereas $\delta^{34}S$ values for both organic and pyritic sulfur in the No. 9 coal seam (which contains more than 3% total sulfur) are more variable and generally tend to be more negative, −12.3 to 5.8‰ and −18.7‰ to 1.1‰, respectively (Table 4). The difference between the maximum and minimum $\delta^{34}S$ values for organic and pyritic sulfur in the No. 9 seam is 18.1‰ and 19.8‰, respectively. The $\delta^{34}S$ values in the No. 13 seam are less variable; the difference between the maximum and minimum $\delta^{34}S$ values for organic and pyritic sulfur is 2.6‰ and 1.1‰, respectively. The relatively uniform isotopic composition of sulfur in low-sulfur coal reflects the uniform isotopic composition of the precursor plant material and freshwater sulfate. The contrasting highly variable isotopic composition of pyritic sulfur in high-sulfur coal indicates that there are probably several generations of pyrite. Isolated microenvironments probably existed in the peat; these microenvironments gave rise to an inhomogeneous distribution of sulfate-reducing bacteria and contributed to the complexity of pyrite formation (Chou, 1990). The existence of rod-like pyritized bacteria and a variety of pyritic distribution patterns, such as framboidal pyrite, euhedral pyrite, massive pyrite, anhedral pyrite, and infiltrational pyrite, suggest several generations of pyrite.

Sulfur isotope compositions observed in the Wuda coals are similar to those of Illinois Basin coals (Price and Shieh, 1979; Westgate and Anderson, 1984) and those of Australian low-sulfur coals (Smith and Batts, 1974), and for all the coals, a large portion of sulfur in high-sulfur coals originates from bacteriogenic sulfide and most of sulfur in low-sulfur coal is preserved from precursor plant materials.

A linear relationship exists between the $\delta^{34}S$ values of pyritic and organic sulfur (Fig. 4a). There is a negative relationship between $\delta^{34}S$ values for organic and pyritic sulfur and total sulfur content (Fig. 4b). Higher $\delta^{34}S$ values are observed in samples that have lower total sulfur content. It is well known that the Fe^{2+} has greater affinity for H_2S than organic material does (Lei and Ren, 1993). Under conditions where $^{32}SO_4^{2-}$ is abundant and bacterial activity is constant, organic matter and H_2S can react to produce organic

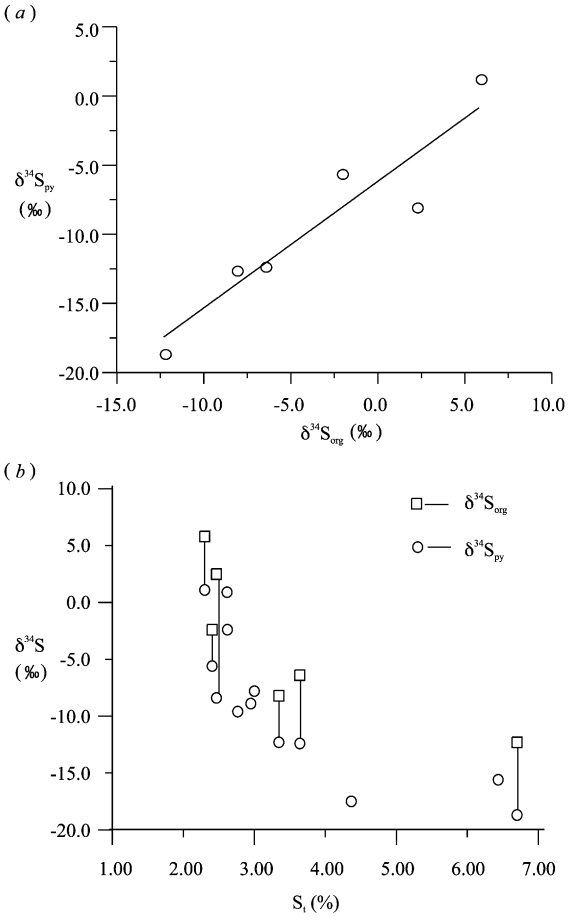

Fig. 4. Distributions of $\delta^{34}S$ values of the No. 9 coal seam. (a) Relationship of the $\delta^{34}S$ values between pyritic and organic sulfur. (b) Relationship of the $\delta^{34}S$ values between organic sulfur and total sulfur content.

sulfur. However, under conditions of limited $^{32}SO_4^{2-}$ availability, both organic matter and Fe^{2+} can incorporate H_2S enriched in ^{34}S content, producing pyrite and organic sulfur with high $\delta^{34}S$ values.

The isotopic behavior of reactant sulfate and product sulfides during bacterial sulfate reduction is easily modeled assuming a constant fractionation factor (Goldhaber and Kaplan, 1979; Lyons et al., 1989). Fig. 5a and b shows the ranges of sulfide and sulfate $\delta^{34}S$ values during prolonged sulfate reduction for situations of unlimited and limited sulfate supplies, respectively. Fig. 5a shows that neither sulfate nor sulfide $\delta^{34}S$ values change with the depth.

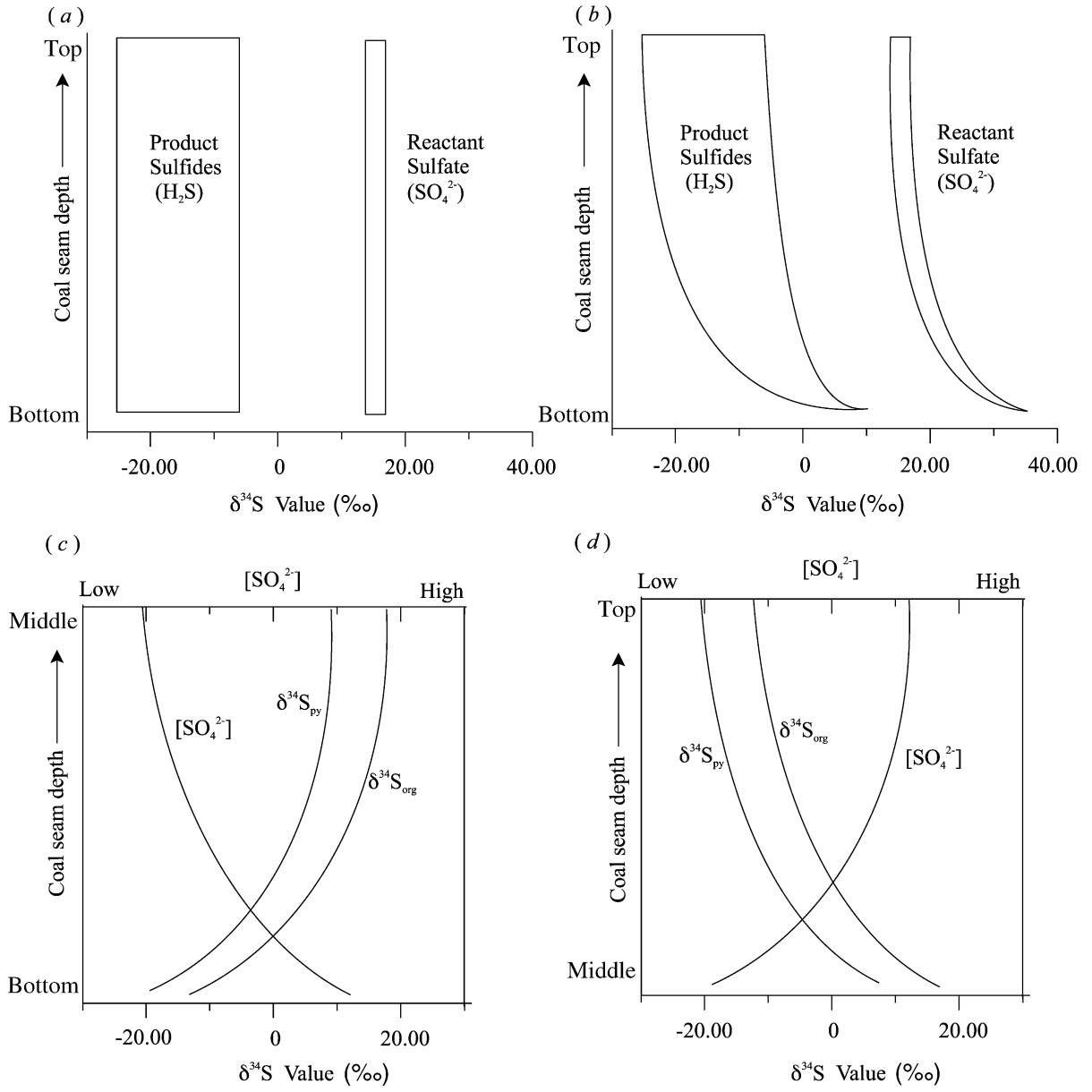

Fig. 5. Model of origin and isotopic composition of sulfur. (a) $\delta^{34}S$ values of sulfate and sulfide versus depth in a system with an unlimited sulfate supply. (b) $\delta^{34}S$ values of sulfate and sulfide versus depth in a system with a limited sulfate supply. (c) Variation of $\delta^{34}S$ in the stage of t1. (d) Variation of $\delta^{34}S$ in the stage of t2.

Based on sulfur isotope compositions and coal petrographic characteristics, a model was developed to explain the origin of sulfur in these coals (see Fig. 5c and d). The changes of the pyrite and organic sulfur content (high on the top and at the bottom plies, low in the middle of the columnar section, see Table 4), and the $\delta^{34}S$ values (light on the top and bottom, heavy in the middle, see Table 4) indicate that there were heavy influences of seawater on peat swamp in early stage (t1) and late stage (t2) of peat accumulation.

In the early stage (t1) (samples from 9-1 to 9-6 with a total thickness of 2.05 m, Table 4), the total sulfur and the pyrite contents of the coal decrease, whereas the pyritic and organic $\delta^{34}S$ values increase markedly. Here, the coal displays features of limited sulfate supply during the late t1. However, the initial sulfide formed from bacterial reduction of an unlimited supply of sulfate (Fig. 5a). At the beginning of t1, enough SO_4^{2-} was available because of strong marine influence, and this weak reducing environment favored bacteria activity. Unlimited sulfate supply produced sulfides about 15–40% lower than the $\delta^{34}S$ values of the initial sulfate because of the open system (Lyons et al., 1989), and thus, resulted in comparatively ^{32}S-rich sulfur species at the bottom of the coal bed. The marine influence gradually diminished with peat accumulating and a limited supply of sulfate with heavy $\delta^{34}S$ leads to product sulfides whose $\delta^{34}S$ values increase with depth during t1. Prolonged transfer of ^{32}S from the sulfate reservoir to the sulfide reservoir increases the sulfate $\delta^{34}S$. This phenomenon provides a clue to a possible origin of the increase in the $\delta^{34}S$ values within the column section during t1 (Fig. 5c).

After the first stage t1, the second stage t2 (samples from 9-7 to 9-13 with a total thickness of 2.29 m) begins. The total sulfur content increases, but the isotopic values of sulfur decrease sharply. This indicates that marine influence became strong. The No. 9 coal seam was overlain by a bay-fill shale roof which indicates marine influences (Peng and Zhang, 1995). Fig. 5d can explain the variation of isotopic values of pyrite and organic sulfur within the column section during t2.

The high contents of total sulfur in basal and top plies could be explained by growth of the peat mire in a transgressive marine setting and inundation of the peat surface by sulfate-rich seawater. The high pyritic sulfur content in top plies would indicate availability of ferrous iron in the peat, following the observations of Casagrande et al. (1977) and Passier et al. (1997). The major difference between Fig. 5c and d is that the directions of $\delta^{34}S$ and $[SO_4^{2-}]$ are opposite. Fig. 5c shows that $[SO_4^{2-}]$ decreases, but $\delta^{34}S$ values increase from the bottom to the middle of the coal seam; whereas Fig. 5d shows that $[SO_4^{2-}]$ concentration increases, but $\delta^{34}S$ values decrease from the middle to the top of the No. 9 coal.

Altschuler et al. (1983) reported that a mount of pyritic sulfur is concentrated mainly in the basal half of peat cores and is highest at the base in Everglades

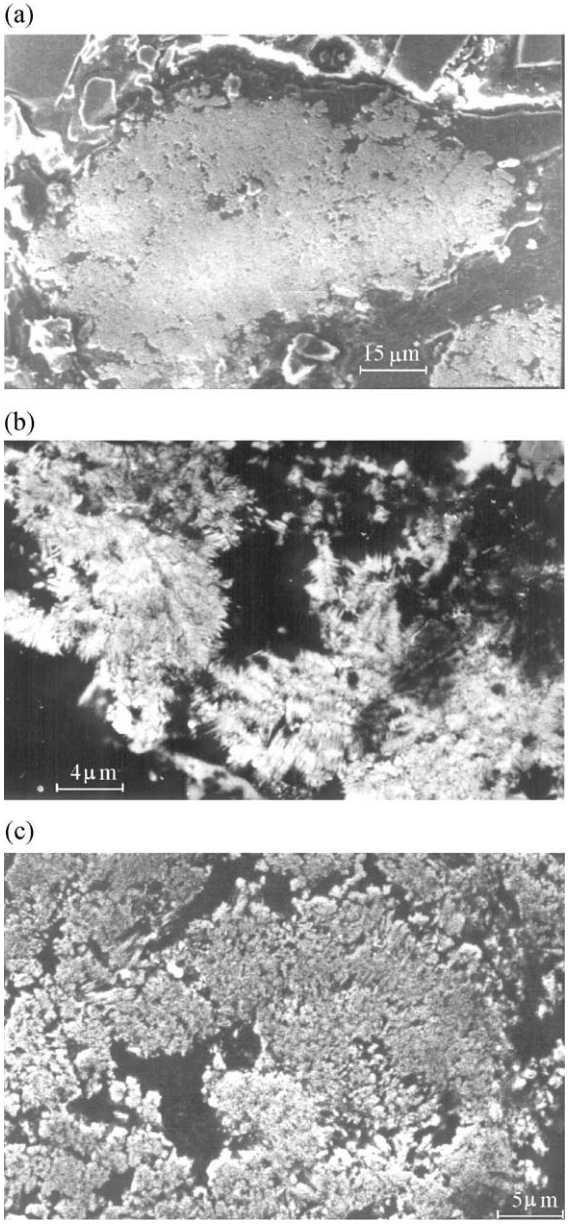

Fig. 6. Characteristics of pyritized rod-like bacteria in the No. 9 coal seam. (a) Particular shape of bacteria with irregular edge (SEM). (b) Individual bodies with spiculate shapes of bacteria (SEM). (c) Fascicular body with radial shape and phase-growth of bacteria (SEM).

freshwater peats. Goldhaber and Kaplan (1980) reported a similar depth-dependent increase in $\delta^{34}S_{py}$ values from modern marine sediments of the Gulf of California. Lyons et al. (1989) studied variations of the pyrite content and isotopic values of the Lower Bakerstown coal with depth. Lei and Ren (1993) found that the $\delta^{34}S$ value of pyrite increases from the bottom ($-30.6‰$) to the top ($-28.2‰$) in the high organic sulfur coals in Guiding, Guizhou Province, South China. All above studies on the isotopic variation and mechanism of sulfur formation are similar. The Wuda coal bed differs from above areas in this important aspect—the $\delta^{34}S$ values of pyrite and organic sulfur increase from the bottom and then decrease to the top of the coal bed.

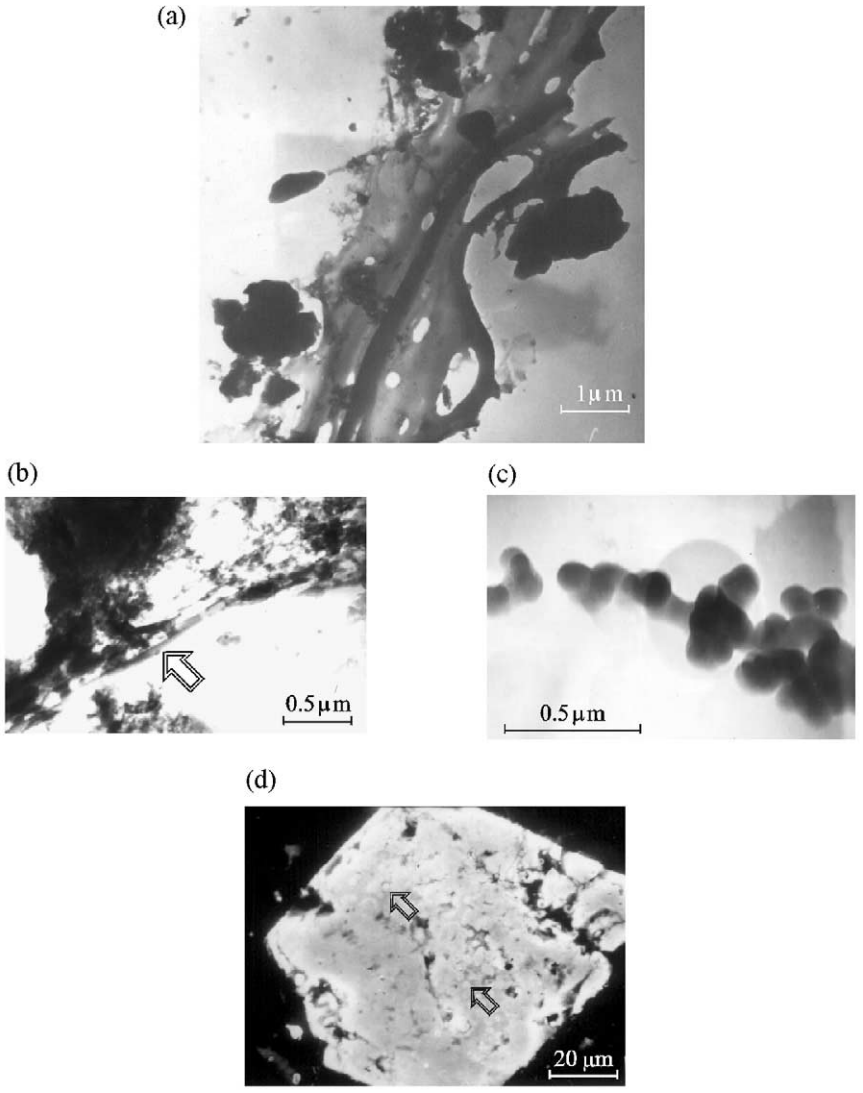

Fig. 7. Characteristics of cyanophyte's gelatinous sheaths and degraded algae organic matter. (a) Gelatinous sheath of filamentous cyanophyte with no cellular structure (TEM). (b) Degraded filamentous cyanophyte with cavity structure (TEM). (c) Mineralized organic matter of algae probably related to blue-green algae (TEM). (d) Mineralized *Chroococacece* colony (SEM).

7. Findings of pyritized rod-like bacteria and degraded algae organic matter

Identification of modern bacteria relies on their shape, size, chemical component, and cultivating characteristics in modern microbiology, whereas mineralized bacterial bodies can only be identified by their size and particular shape (Lei et al., 1995). Pyritized rod-like bodies in the No. 9 coal seam have been identified as bacteria using SEM-EDX evidences: (1) their particular shape of bacteria with irregular edge (Fig. 6a), (2) individual bodies with spiculate shapes (Fig. 6b), (3) fascicular bodies with radial shape and phase-growth (Fig. 6c), (4) most cells of individual bodies with the size under 1 μm, (5) the total bacterial clusters with only about 100 μm. The rod-like bacteria identified here with SEM-EDX are pyritized.

During peat accumulation of the No. 9 coal seam, much SO_4^{2-} was supplied because of the seawater influence. The weak reducing and alkaline environment favored bacterial action and propagation, producing abundant H_2S that reacted with ferrous iron to form pyrite and with organic peat compounds to form organic sulfur compounds. H_2S in seawater can be produced only by bacterial actions, because there is not enough energy for the conversion from sulfate to sulfide by pure chemical reactions (Dai et al., 1998). Moreover, the fact that the sulfur isotope values of organic and pyritic sulfur in the No. 9 coal seam are relatively low indicates that there was vigorous bacteria activity during peat accumulation. Another evidence for the strong bacteria activity is the high collodetrinite and low telinite content since the bacteria can decompose organic materials under the condition of reducing and alkaline environment (Shimoyama et al., 1990).

Several kinds of the cyanophyte's gelatinous sheaths and degraded organic matter in collotelinite in the No. 9 coal seam have been found using TEM. They revealed the following characteristics: (1) gelatinous sheath of filamentous cyanophyte with no cellular structure (Fig. 7a), (2) degraded organic matter of filamentous cyanophyte with cavity structure (Fig. 7b), (3) mineralized organic matter of algae is probably related to blue-green algae (Fig. 7c), (4) mineralized *Chroococacece* colony with the crystal form of calcite, the pyritic composition determinated by SEM-EDX, and many globular cells inside it (Fig. 7d). Algae can play an important role in enriching elements, changing pH and Eh values during their life activity and degradation after their death (Liu, 1996). Algae may have provided sulfur and nutrient to the sulfate reducing bacteria during the anaerobic decomposition of the peat as well as increasing the amount of ferrous iron. If so, then the present distribution of sulfur in these coals may correspond to past contributions of algae to the coal-forming peat.

8. Conclusions

Based on the petrographic characteristics, abundance, distribution, and isotopic variation of sulfur in coals in Wuda coalfield, the following conclusions can be drawn from the data and discussion in this paper.

(1) The high-sulfur coals in the Wuda coalfield are dominated by vitrinite group macerals with average content being 70.8%. The high content of collodetrinite indicates a strong gelification during peat accumulation. The coal seams formed in fluvial delta plain have high mineral contents, especially the clay minerals.

(2) Results from the analysis of the organic sulfur in individual macerals showed that the organic sulfur content in macerals in coals formed in different depositional environments decreases in order of tidal delta plain>tidal flat>fluvial delta plain. Collodetrinite has the highest organic sulfur content and fusinite has the least in coals from the same sample. There is a positive relationship between organic sulfur content in collodetrinite and the vitrinite group content because the precursors of vitrinite group formed where the water table in peat-forming environment was high and Eh was low.

(3) $\delta^{34}S$ values of organic and pyritic sulfur suggested that a large portion of sulfur in high-sulfur coal (No. 9 coal seam) originates from bacteriogenic sulfide and most of sulfur in low-sulfur coal (No. 13 coal seam) is preserved from precursor plant materials. The vertical variation of $\delta^{34}S$ values of sulfur showed that there were strong seawater influences in early t1 and late t2 during peat accumulation.

(4) Numerous pyritized rod-like bacteria and degraded algae organic matter have been found in

high-sulfur coal (No. 9 coal seam). It is believed that bacteria, and perhaps algae, may play an important role in the formation of these high-sulfur coals.

Acknowledgements

This research was supported by the National Natural Science Foundation of China (No. 40072054), the Coal Science Foundation of China (No. 97Geo-10205). We would like to thank Dr. Robert B. Finkelman, Dr. Chenlin Chou, Dr. Paul. C. Lyons and Prof. V. Bouska for their constructive discussion. The authors are grateful to Prof. Zhili Liu and Prof. Lizeng Bian for their identification of degraded algae organic matter and pyritized rod-like bacteria. We thank the personnel of the Wuda Coal Bureau, especially Mr. Fengxue Ma and Mr. Baochun Li, who supplied support while sampling underground and for the much useful information. In addition, we appreciate the help of personnel at China University of Mining and Technology, especially Prof. Dexin Han, a member of Chinese Academy of Engineering, Prof. Pengfei Zhang, Ms. Huimin Hou and Mr. Tianjie Ai. Special appreciation is expressed to Ms. Yurong Liu for designing computer programs used in this study.

References

Altschuler, Z.S., Schnepfe, M.M., Silber, C.C., Simon, F.O., 1983. Sulfur diagenesis in Everglades peat and origin of pyrite in coal. Science 221, 221–227.

ASTM (American Society for Testing and Materials), 1997. Annual Book of ASTM Standards. Gaseous Fuels: Coal and Coke, vol. 05.05. ASTM, Philadelphia, PA.

Casagrande, D.J., 1987. Sulfur in peat and coal. In: Scott, A.C. (Ed.), Coal and Coal-bearing Strata: Recent Advances, vol. 32. Geological Special Publication, London, pp. 87–105.

Casagrande, D.J., Price, F.T., 1981. Sulfur isotope distribution in coal precursors. Abstracts with Programs-Geological Society of America 13, 423–424.

Casagrande, D.J., Siefert, K., Berschinski, C., Sutton, N., 1977. Sulfur in peat-forming systems of Okefenokee swamp and Florida everglades: origin of sulphur in coal. Geochimica et Cosmochimica Acta 41, 161–167.

Chou, C.-L., 1990. Geochemistry of sulfur in coal. In: Orr, W.L., White, C.M. (Eds.), Geochemistry of Sulfur in Fossil Fuels. American Chemical Society, Washington, DC, Symposium Series, vol. 429, pp. 30–52, Chap. 2.

Chou, C.-L., 1997. Geological factors affecting the abundance, distribution, and speciation of sulfur in coals. In: Yang, Q. (Ed.), Geology of Fossil Fuels—Coal. Proceedings of the 30th International Geological Congress, vol. 18, Part B. VSP, Utrecht, The Netherlands, pp. 47–57.

Dai, S., 2000. The action and significance of low organism in the formation of high-sulfur coal. Scientia Geologica Sinica 9 (3), 339–352.

Dai, S., Ren, D., 1996. Distribution of organosulfur in macerals of coals in the Wuda mining area. Coal Geology of China 18, 20–24 (in Chinese with English abstract).

Dai, S., Ren, D., Tang, Y., Hou, H., Mao, H., 1998. The evolution and characteristic of peat swamp in the Wuda coalfield. Journal of Coal Society 23, 7–11 (in Chinese with English abstract).

Demir, I., Harvey, R.D., Hackley, K.C., 1993. SEM-EDX and isotope characterization of the organic sulfur in macerals and chars in Illinois Basin coals. Organic Geochemistry 20, 257–266.

Diessel, C.F.K., 1992. Coal-bearing Depositional Systems. Springer, Berlin, p. 721.

Gayer, R.A., Rose, M., Dehmer, J., Shao, L.-Y., 1999. Impact of sulphur and trace elements geochemistry on the utilization of a marine-influenced coal-Case study from the South Wales Variscan forland basin. International Journal of Coal Geology 40, 151–174.

Goldhaber, M.B., Kaplan, I.R., 1979. The sulfur cycle. In: Goldberg, E.D. (Ed.), The Sea, vol. 5. Wiley, New York, pp. 569–655.

Goldhaber, M.B., Kaplan, I.R., 1980. Mechanisms of sulfur incorporation and isotope fractionization during early diagenesis in sediments of the Gulf of California. Marine Chemistry 9, 95–143.

Han, D., Yang, Q. (Eds.), 1980. Coal Geology of China, vol. 2. Publishing House of China Coal Industry, Beijing (in Chinese).

Kostava, I., Petrov, O., Kortenski, J., 1996. Mineralogy, geochemistry and pyrite content of Bulgarian subbituminous coals, Pernik Basin. In: Gayer, R., Harris, I. (Eds.), Coalbed Methane and Coal Geology, vol. 109. Geological Society Publication, London, pp. 301–314.

Lei, J., Ren, D., 1993. The petrological and geochemical characteristics of Permian high organosulfur coal from Guiding, China. In: Parekh, B.K., Groppo, J.G. (Eds.), Processing and Utilization of High-Sulfur Coals V. Elsevier, Amsterdam, pp. 27–35.

Lei, J., Ren, D., 1995. The distribution of organic sulfur of coals formed in different accumulating environments. Coal Geology & Exploration 23 (6), 14–18 (in Chinese with English abstract).

Lei, J., Pu, Y., Ren, D., 1995. Bacterium-like bodies and its significance in high organosulfur coal from Guiding. Acta Petrolei Sinica 11, 456–461 (in Chinese with English abstract).

Liu, G., 1990. Permo-Carboniferous paleography and coal accumulation and their tectonic control in North China and South China continental plates. International Journal of Coal Geology 16, 73–117.

Liu, Z., Li, P., 1996. A simulation test of copper ore biomineralization by the algae. In: Ye, L. (Ed.), Bio-organic Mineralization. Oceanic Publishing House, Beijing, pp. 198–206 (in Chinese).

Love, L.G., Coleman, M.L., Curtis, C.D., 1983. Diagenetic pyrite formation and sulphur isotope fractionation associated with a Westphalian marine incursion, northern England. Transactions

of the Royal Society of Edinburgh. Earth Sciences 74, 165–182.

Lyons, P.C., Whelan, J.F., Dulong, F.T., 1989. Marine origin of pyritic sulfur in the Lower Bakerstown coal bed, Castleman coal field, Maryland (U.S.A.). International Journal of Coal Geology 12, 329–348.

Mastalerz, M., Bustin, R.M., 1993. Variation in elemental composition of macerals: an example of the application of electron microprobe to coal studies. International Journal of Coal Geology 22 (1), 83–99.

Passier, H.F., Middelburg, J.J., de Lange, G.J., Bottcher, M.E., 1997. Pyrite contents, microtextures, and sulfur isotopes in relation to formation of the youngest eastern Mediterranean sapropel. Geology 25, 519–522.

Peng, S., Zhang, J., 1995. The Coal-Bearing Depositional Environment and its Influence to Mining of the Wuda Coalfield Publishing House of China Coal Industry, Beijing (in Chinese).

Price, F.T., Casagrande, D.J., 1991. Sulfur distribution and isotopic composition in peats from the Okefenokee Swamp, Georgia and the Everglades, Florida. International Journal of Coal Geology 17, 1–20.

Price, F.T., Shieh, Y.N., 1979. The distribution and isotopic composition of sulfur in coals from the Illinois basin. Economic Geology Bulletin, Society of Economic Geology 74, 1445–1461.

Raymond, R., 1978. The distribution of organic sulfur in American coal. Scanning Electron Microscopy 1, 93–108.

Shimoyama, T., Yamazaki, K., Iijima, A., 1990. Sulphur isotopic composition in the Palaeogene coal of Japan. International Journal of Coal Geology 15, 191–217.

Smith, J.W., Batts, B.D., 1974. The distribution and isotopic composition of sulfur in coal. Geochimica et Cosmochimica Acta 38, 121–133.

Smith, J.W., Gould, K.W., Rigby, D., 1981. The stable isotope geochemistry of Australian coals. Organic Geochemistry 3, 111–131.

Spiker, E.C., Pierce, B.S., Bates, A.L., Stanton, R.W., 1994. Isotopic evidence for the source of sulfur in the Upper Freeport Coal Bed (west-central Pennsylvania, U.S.A.). Chemical Geology 114, 115–130.

Tang, Y., Ren, D., 1993. Research on different pyrites in Late Permian coal of Sichuan Province, Southwest China. In: Parekh, B.K., Groppo, J.G. (Eds.), Processing and Utilization of High-Sulfur Coals V. Elsevier, Amsterdam, pp. 37–46.

Ward, C.R., Gurba, L.W., 1998. Occurrence and distribution of organic sulphur in macerals of Australian coals using electron microprobe techniques. Organic Geochemistry 28 (11), 635–647.

Westgate, L.M., Anderson, T.F., 1984. Isotopic evidence for the origin of sulfur in the Herrin (No. 6) Coal member of Illinois. International Journal of Coal Geology 4, 1–20.

Whateley, M.K.G., Tuncali, E., 1995. Origin and distribution of sulphur in the Neogene Beypazari Lignite Basin, Central Anatolia, Turkey. In: Whateley, M.K.G., Spears, D.A. (Eds.), European Coal Geology, vol. 82. Geological Society Special Publication, London, pp. 307–323.